ELSEVIER

Contents lists available at ScienceDirect

Journal of Solid State Chemistry

journal homepage: www.elsevier.com/locate/jssc



Cerium luminescence in nd^0 perovskites

A.A. Setlur a,*, U. Happek b

- ^a GE Global Research Center, 1 Research Circle, Niskayuna, NY 12309, USA
- ^b Department of Physics and Astronomy, University of Georgia, Athens, GA 30602, USA

ARTICLE INFO

Article history: Received 14 December 2009 Accepted 17 March 2010 Available online 20 March 2010

Keywords: Perovskites Ce³⁺ Luminescence

ABSTRACT

The luminescence of Ce^{3+} in perovskite (ABO₃) hosts with nd^0 B-site cations, specifically $Ca(Hf,Zr)O_3$ and (La,Gd)ScO₃, is investigated in this report. The energy position of the Ce^{3+} excitation and emission bands in these perovskites is compared to those of typical Al^{3+} perovskites; we find a Ce^{3+} 5d¹ centroid shift and Stokes shift that are larger versus the corresponding values for the Al^{3+} perovskites. It is also shown that Ce^{3+} luminescence quenching is due to Ce^{3+} photoionization. The comparison between these perovskites shows reasonable correlations between Ce^{3+} luminescence quenching, the energy position of the Ce^{3+} 5d¹ excited state with respect to the host conduction band, and the host composition.

© 2010 Elsevier Inc. All rights reserved.

1. Introduction

The relative simplicity of the Ce³⁺ energy levels has led to phenomenological models for the position of the 5d¹ centroid and the crystal field splitting of the 5d¹ levels [1,2]. There are also empirical rules to understand the parameters for Ce³⁺ photoionization quenching, starting with a minimum host bandgap for efficient Ce³⁺ luminescence in oxides [3] with further work towards understanding the position of the Ce³⁺ 4f¹ ground state within the host lattice bandgap [4]. This work to quantify and understand Ce³⁺ luminescence has practical implications since Ce³⁺ luminescence is used in many efficient phosphors and scintillators, and additional progress towards the relationship between host composition and Ce³⁺ luminescence could lead to insight for the design of these materials.

One approach to understand host lattice effects on luminescence is to analyze the luminescence properties versus composition for a set of isostructural hosts [5]. For Ce^{3+} luminescence, the ABO₃ perovskites could be instructive for comparisons with compositional variations of the larger A cation and the smaller, octahedral B cation (with a caveat for distortions in the octahedral arrays for different A/B combinations). Prior work in Al^{3+} perovskites has studied the effect of composition on the energy position of the Ce^{3+} $4f^1 \rightarrow 5d^1$ transitions [1] as well as photoionization quenching [6,7]. We expand upon this prior work by studying Ce^{3+} luminescence in perovskite hosts that have B-site cations with nd^0 configurations, specifically LaScO₃, GdScO₃, CaHfO₃, and CaZrO₃. Using the relationship between the average

cation electronegativity and A–O bonding in perovskites and the Ce³+ 5d¹ centroid shift and crystal field splitting [1,2], it is possible to correlate the perovskite composition to the energy position of the lowest Ce³+ 4f¹ → 5d¹ transition. In regard to the Ce³+ luminescence quenching, while the absorption edge of these perovskites are at relatively low energies (<5.9 eV) [8,9], there are significant differences in the thermal quenching of the 5d¹ → 4f¹ Ce³+ luminescence. A Born–Haber method [10] is used to analyze the photoionization thresholds and gives a qualitative correlation between the Ce³+ luminescence efficiency and perovskite composition. Therefore, we demonstrate systematic compositional trends in these perovskites for both the energy position of the lowest Ce³+ 5d¹ level and photoionization quenching of Ce³+ luminescence.

2. Experimental procedure

Standard solid-state synthesis methods using high purity $CaCO_3$, La_2O_3 , Gd_2O_3 , Lu_2O_3 , Sc_2O_3 , HfO_2 , ZrO_2 , and CeO_2 were used to make powder samples. Ce^{3+} ions replace the larger A-site cations at nominal levels of 0.1–1%, and for $Ca(Hf,Zr)O_3$, there is no intentional charge compensation. The compositions reported here are nominal compositions and all samples are single-phase orthorhombic perovskites as determined by powder X-ray diffraction with the exception of $LaScO_3$ that has a trace (< 5%) of unreacted La_2O_3 . However, La_2O_3 : Ce^{3+} does not have any luminescence at liquid He temperatures [3] and should not interfere with the luminescence studies reported here.

Excitation and emission spectra were measured using a Spex Fluoromax 2 spectrofluorometer with a closed cycle He cryostat that has a cold finger attachment. Diffuse reflectance

^{*} Corresponding author. Fax: +15183876204. E-mail address: setlur@ge.com (A.A. Setlur).

measurements used the same spectrometer with BaSO₄ (Kodak) as a reflectance standard. Time resolved measurements from 77 to 450 K used a LED excitation source filtered through a narrow band interference filter (10 nm width) driven by the amplified (Avantec) pulses of an Avtech AVP-C pulse generator. The emission was filtered through a 0.5 m McPherson monochromator and detected with a Hamamatsu R212 PMT detector. The time resolved fluorescence was recorded through a photon counting system consisting of an Ortec 567 time-to-amplitude converter in conjunction with an EG & G pulse height analyzer. The temporal response for this experimental setup was measured at 2 ns. Time resolved measurements above 300 K also used powder pressed into a Al plaque with cartridge heaters, thermocouples, and a Watlow temperature controller and a tripled Nd:YAG laser at 355 nm (JDS Uniphase) coupled into an Edinburgh F900 spectrofluorometer with a Peltier cooled R928-P Hamamatsu photomultiplier tube (PMT) detector. The FWHM of the laser pulse convoluted with the overall system response is ~ 1 ns. Measurements of the thermoluminescence excitation spectra (TLES) followed previously reported procedures [11].

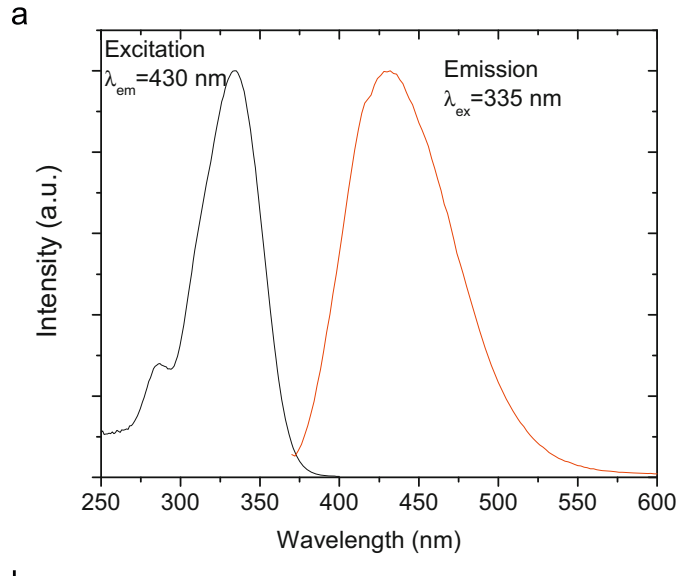
3. Results and discussion

3.1. Luminescence of CaHfO₃:Ce³⁺ and CaZrO₃:Ce³⁺

The emission and excitation of CaHfO₃:Ce³⁺ are indicative of typical Ce³⁺ luminescence with a doublet emission band consisting that can be fit by two Gaussians separated by $\sim 2000\,\mathrm{cm}^{-1}$ with $\lambda_{max}{\sim}430\,\text{nm}$ (Fig. 1a). The maximum of the excitation band is at $\sim 335 \,\mathrm{nm}$ ($\sim 29\,900\,\mathrm{cm}^{-1}$) giving a Stokes shift of \sim 6700 cm⁻¹. When accounting for the \sim 12240 \pm 750 cm⁻¹ energy difference between the lowest energy $Ce^{3+} 4f^1 \rightarrow 5d^1$ and $Pr^{3+} 4f^2 \rightarrow 4f^15d^1$ transitions [12], the position of the CaHfO₃:Ce³⁺ excitation band reported here is in reasonable correlation with the position of the main Pr³⁺ excitation band in CaHfO₃ $(\sim 41700\,\mathrm{cm}^{-1})$ [13]. In addition, the Stokes shift for Ce^{3+} and $Pr^{3+} 4f^{N-1}5d^{1} \rightarrow 4f^{N}$ emission is similar (6700 cm⁻¹ for Ce³⁺ vs. $7600\,\mathrm{cm^{-1}}$ for $\mathrm{Pr^{3+}}$) as expected. The Stokes shift for $\mathrm{Ce^{3+}}$ luminescence is also larger in comparison to the Al3+ perovskites but is similar to the Stokes shift for LaLuO3:Ce3+ [14] (Table 1), indicating a potential relationship between the B-site cation size and the Ce³⁺ Stokes shift. The energy position of the lowest Ce³⁺ 5d¹ level in CaHfO₃ is lower when compared to the Al³⁺ perovskites (Table 1); this is primarily due to the lower electronegativity of both Hf⁴⁺ and Ca²⁺ versus Al³⁺ and the trivalent lanthanides [15], respectively. The lower average cation electronegativity increases the O2- anion polarizability and the covalency of the Ce³⁺-O²⁻ bond (via an inductive effect), leading to a larger Ce³⁺ 5d¹ centroid shift [2].

In spite of the low energy position of the absorption edge and the relatively large Stokes shift, CaHfO₃:Ce³⁺ has weak thermal quenching at room temperature (Figs. 1b and 2), and initial measurements of the quantum efficiency ($\lambda_{\rm ex}\sim335\,{\rm nm}$) at room

temperature is $\sim 30\%$ of a standard BaMgAl₁₀O₁₇:Eu²⁺ blue phosphor, a reasonably high value for unoptimized samples. As the initial decay time of CaHfO₃:Ce³⁺ begins to decrease, the decay profile deviates from a single exponential with an additional weak component that has a decay time of > 30 ns, slower than the radiative decay rate (Fig. 1b). This slower decay component is assigned to an afterglow luminescence that occurs after charge carriers are created, trapped at defects, and slowly detrapped from those defects. The correlation between the



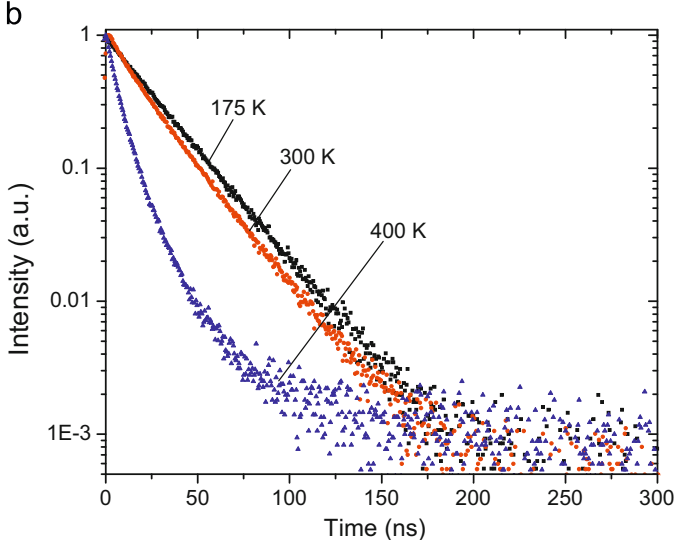


Fig. 1. (a) Emission (λ_{ex} =335 nm) and excitation spectra of (λ_{em} =430 nm) of Ca_{0.99}Ce_{0.01}HfO₃ at \sim 10 K and (b) Decay profiles (λ_{ex} =320 nm, λ_{em} =440 nm) versus temperature for Ca_{0.999}Ce_{0.001}HfO₃. The background has been subtracted from these decay profiles.

Table 1 Emission and excitation peaks for Ce³⁺-doped perovskites.

Host	Excitation (cm ⁻¹)	Emission (cm ⁻¹)	Stokes shift (cm ⁻¹)	Reference
CaHfO ₃	29 900	23 200	6700	This work
LaScO ₃	30 950	23 300	7700	This work
GdScO ₃	28 650	23 300	5350	This work
YAlO ₃	33 000	28 500	4500	[26]
GdAlO ₃	32 500	29 590	2900	[27]
LaAlO ₃	31 750	No emission		[6]
LaLuO ₃	29 850	22 400	7450	[12]

Download English Version:

https://daneshyari.com/en/article/1332607

Download Persian Version:

https://daneshyari.com/article/1332607

<u>Daneshyari.com</u>